

THE SELF-POTENTIAL RESPONSE DURING HYDRAULIC FRACTURING OF SIERRA GRANITE

Jeffrey R. Moore
Steven D. Glaser

University of California, Berkeley
Department of Civil and Environmental Engineering
440 Davis Hall
Berkeley, CA USA
e-mail: moore@ce.berkeley.edu

ABSTRACT

The self-potential (SP) response during hydraulic fracturing of intact Sierra granite specimens was investigated in the laboratory. Excellent correlation of injection pressure and SP suggests that the SP response is created primarily by electrokinetic coupling. For low injection pressures the variation of SP and pressure drop is linear indicating a constant coupling coefficient (C_c). However, for injection pressures $>2\text{MPa}$ the C_c increases with pressure by nearly 80% in an exponential trend. The increasing C_c is likely related to increasing permeability at high pore pressures due to dilatancy of micro-cracks.

INTRODUCTION

The self-potential (SP) method is a passive geophysical tool in which naturally occurring voltages are measured with changing space or time. The SP response during *tensile* fracturing of earth materials and hydraulic fracturing have received little attention from previous researchers. Wurmstich (1995) showed numerical results suggesting that the process of hydraulic fracturing augments the SP signal by up to an order of magnitude. Pritchett and Ishido (2005) recently performed numerical simulations concluding that large SP anomalies are created during hydraulic fracturing which could be easily detected by downhole monitoring. Grinat et al. (2004) monitored the surface SP response during field stimulations at a depth of 3790m and observed no correlation between the SP anomalies and injection events. On the contrary, Kawakami and Takasugi (1994) and Marquis et al. (2002) reported surface SP data during hydraulic stimulation of deep hot dry rock reservoirs, demonstrating good correlation between the temporal SP variation and injection pressure and flow rate. Surface anomalies up to 40 mV correlate to both injection and flow-back events.

ELECTROKINETIC PHENOMENA

Electrokinetic phenomena arise from movement of ions in the electric double layer under a pore pressure gradient. Fluid flow causes mobile ions to be convected relative to the bound charge on the mineral grain surfaces; charge motion known as the convection current. As this charge is deposited in the direction of flow, and the bound charge is left exposed at the flow source, a charge separation exists which drives an Ohmic return current, or the conduction current. In the absence of external current sources the convection current and conduction current are equal and opposite, and equating them reveals the classic result of Smoluchowski (1903):

$$\Delta\phi = C_c \cdot \Delta p \quad (1)$$

$$C_c = \frac{\Delta\phi}{\Delta p} = \frac{\epsilon\zeta}{\eta F_o \sigma_b} \quad (2)$$

$$\text{where: } \sigma_b \cong \frac{\sigma_f}{F_o} + \sigma_s \quad (3)$$

C_c is known as the streaming potential coupling coefficient. Here, η is the dynamic fluid viscosity, ϵ is the absolute dielectric constant of the fluid, σ_b is the bulk sample conductivity, σ_f is the fluid conductivity, σ_s is the surface conductivity, F_o is the electrical formation factor, and ζ is the zeta potential, which is a measure of how much charge resides in the diffuse part of the electric double layer. Equation 2 relies on the assumptions that fluid flow is laminar and that the geometry of the hydraulic and electrical flows is identical, assumptions which may be violated when considering hydraulic fracturing of intact crystalline rocks (Morgan et al., 1989; Lorne et al., 1999).

EXPERIMENTAL

The test specimens were 57 mm diameter, 102 mm long cores of Sierra granite taken from the same block. A 6.35 mm diameter axial hole was drilled to within 25 mm of the bottom of each specimen. This hole was then over-cored at 9.53 mm diameter for 25 mm from the top of the sample to create a vertical exposed bore length of 50 mm in the sample center. Next, the injector was prepared by machining a groove in 6.35 mm OD stainless steel tubing, which accepted a silicon o-ring. The injector was placed into the borehole so that the o-ring sat upon the lip created by the over-coring, and the space around the steel tubing and above the o-ring was filled with a non-conducting epoxy. The sample was then placed in an oven at 150°C for at least 12 hours to cure the epoxy and eliminate any pore fluid left over from drilling. Figure 1 illustrates the sample configuration.

Self-potentials were recorded on six 13 x 22 mm Ag/AgCl electrodes spaced 25 mm around the circumference of the sample. The reference electrode for SP measurements was a 25 mm bare wire end located in the center of each core (Figure 1). Voltage measurements were recorded at 5kHz, while injection pressure was recorded on an independent acquisition system at 10 Hz.

The samples were wetted with water by placing them under vacuum and 2 m head for at least 48 hours. The pore fluid used for all testing was 0.001M NaCl solution ($\rho_f = 75 \Omega\cdot\text{m}$). Injectate was applied to the specimens at a constant rate of 0.154 ml/s via an injection pump.

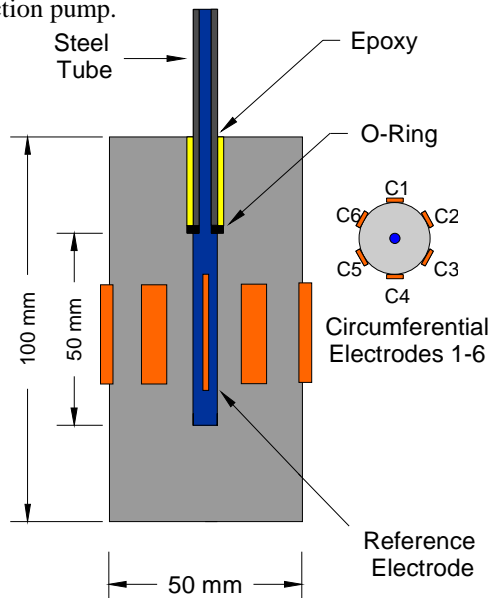


Figure 1: Schematic of Sierra granite test specimens.

RESULTS

The Sierra granite specimens were hydraulically fractured by applying water to the sample center at a constant rate. Excellent correlation of injection pressure and SP suggests that the SP response is created primarily by electrokinetic coupling (Figures 2a, 3a). For low injection pressures the variation of SP and pressure drop is linear indicating a constant C_c (Figure 2b), where the C_c is calculated as the local slope of the SP versus injection pressure curve. However, for injection pressures $>2\text{MPa}$ the C_c increases with pressure (Figure 3b). Figure 4 shows data from 7 samples of Sierra granite demonstrating that the C_c increases by nearly 80% in an exponential trend for injection prior to hydraulic fracturing.

Previous researchers have reported that for high fluid velocities flow separation can occur causing a change in the C_c (Middleton, 1997). Due to the very low hydraulic conductivity of the Sierra granite specimens, fluid flow (prior to fracturing) remains laminar even at high injection pressure, where the maximum Reynolds number is on the order of 10^{-3} .

After fracturing, the SP continues to mimic the injection pressure as the pressure declines and stabilizes (Figure 3b). These results demonstrate that SP may be used as a proxy for fluid pressure when pressure cannot be directly measured.

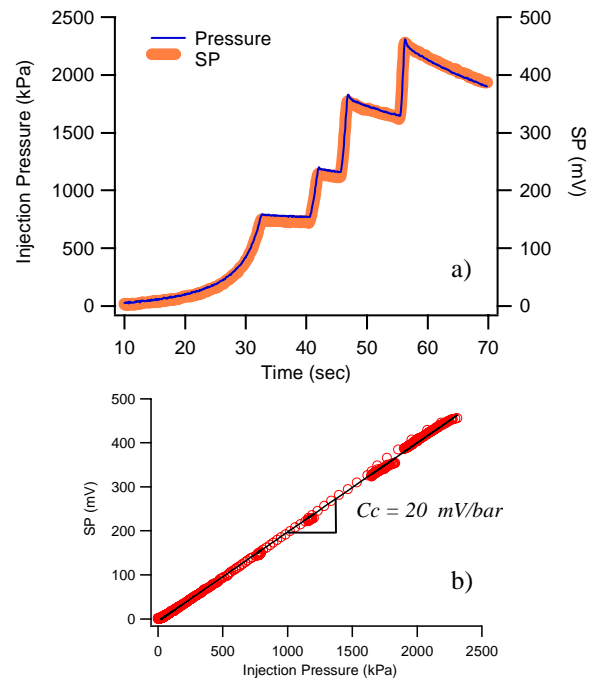


Figure 2: a) Injection pressure and SP response for low-pressure testing prior to hydraulic fracturing, b) linear variation of SP with injection pressure indicates a constant C_c for pressures $< \sim 2 \text{ MPa}$.

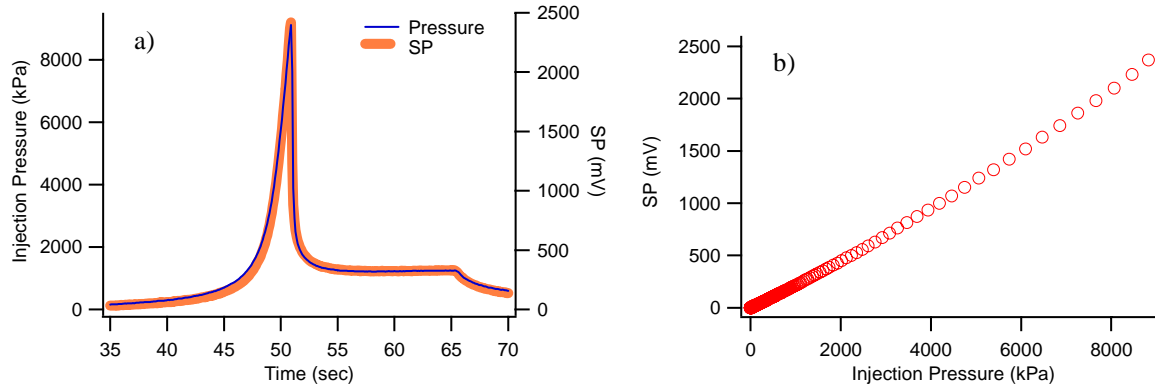


Figure 3: a) Injection pressure and SP response during hydraulic fracturing, b) variation of SP with injection pressure for times preceding fracturing. Here the variation is non-linear revealing an increasing C_c with increasing injection pressure.

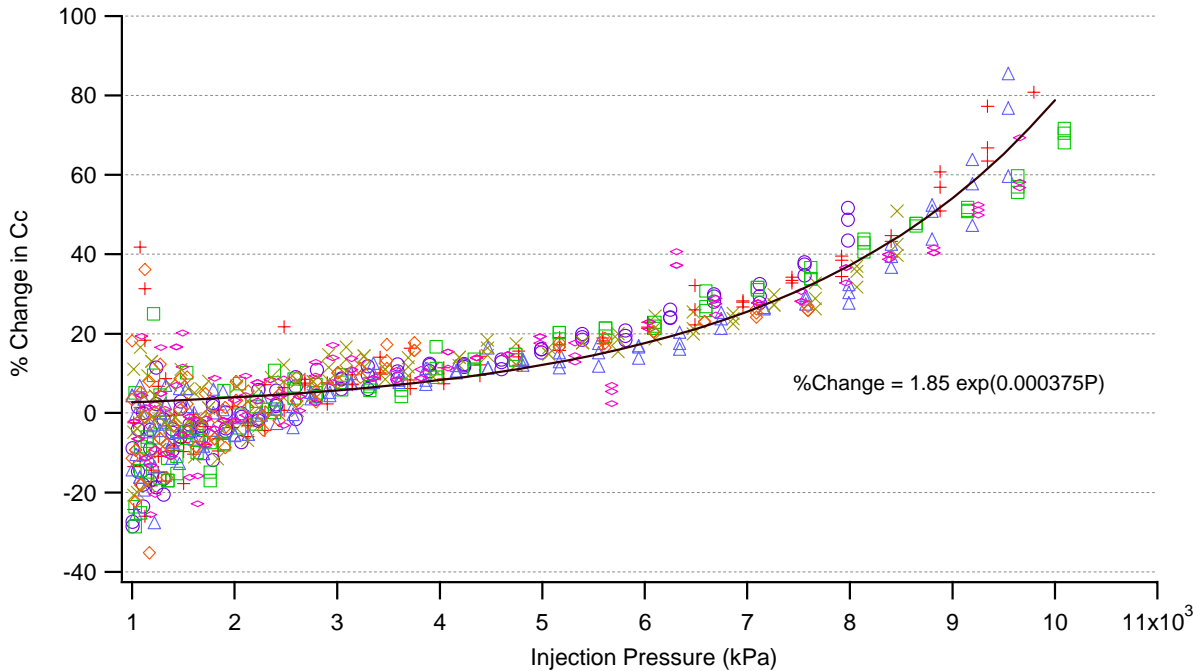


Figure 4: Variation of the C_c with injection pressure for 7 samples of Sierra granite. The C_c increases exponentially with injection pressure, up to 80% just prior to hydraulic fracturing. The best fit line (solid) to all data is shown along with the numerical expression. (Specimen legend: SG2-plus, SG3-circle, SG4-square, SG5-triangle, SG6-diamond, SG7-oval, SG8-cross)

DISCUSSION

The C_c measured here is the change in observed voltage for a change in the injection pressure. Since the pressure on the outside of the sample is atmospheric, the injection pressure is the pressure drop across the radius of the sample. Since the sample configuration creates radial flow of both fluid and current, the C_c is measured in an unconventional way. Traditionally, the C_c is determined using cylindrical core specimens where flow is axial, and fluid pressure and voltage are monitored on each end of the sample. Both electrical and fluid flows occur

through the same cross-sectional area, so by analogy to a capillary tube we can use Equation 2 (Morgan et al., 1989). In this testing, we similarly measure the voltage and fluid pressure drop from the flow source in the center of the specimen radial to the sample edge, and intuitively the electric and hydraulic flows occupy nearly the same area making the geometrical constant of the flows similar.

The C_c measured here is about one order of magnitude higher than that measured for intact Westerly granite (Reppert and Morgan, 2003), and about 3 times larger than that measured for intact Inada granite (Tosha et al., 2003). We measured the

Cc for Sierra granite in the 'traditional' (axial/cylindrical) way and found that it is 17 mV/bar, in good agreement with the value of 20 mV/bar measured using the radial method.

The increasing Cc is likely related to increasing permeability at high pore pressures due to dilatancy of micro-cracks. Previous research has shown an increased Cc with increasing permeability (Jouniaux and Pozzi, 1995; Lorne et al., 1999). Bernaix (1969) investigated the permeability variation with pore pressure gradient for various pressure-sensitive materials concluding that at high pore pressure permeability can increase by orders of magnitude.

Jouniaux and Pozzi (1995) argue that changes in the Cc during deformation are created by variations in the effect of surface conductivity. Specifically, at greater permeability the surface conductivity is reduced, since it is directly related to the pore size, and the electrical gradient increases to equilibrate the convection current. Increasing the electrical gradient for the same pressure gradient results in a larger Cc.

Lorne et al. (1999) however, propose that competing changes in the electrical and hydraulic tortuosities result in a net increased Cc during dilatancy. In their model, the Cc is directly related to a geometrical factor which is the ratio of the electrical to the hydraulic tortuosity. During dilatancy, the electrical tortuosity increases faster than the hydraulic tortuosity as the finer scale cracks that make up the electrical network open and are connected. This results in an increased Cc.

Other variables which affect the Cc include: a) specimen resistivity, which decreased by only a few percent, b) zeta potential, which may increase as new surface area is exposed (Jouniaux and Pozzi, 1995), c) increased viscosity by electroviscous effects.

CONCLUSION

We have investigated the self-potential response during hydraulic fracturing by conducting a series of experiments in the laboratory. We fractured Sierra granite cores by applying water at a constant rate to the sample center. Electrodes on the perimeter monitored the temporal SP response, which closely mimicked the injection pressure suggesting an electrokinetic source mechanism. For low injection pressures the Cc is constant, however for injection pressures >2MPa the Cc increases with pressure by nearly 80% in an exponential trend. The increasing Cc is likely related to increasing permeability at high pore pressure.

REFERENCES

- Bernaix, J. (1969), New laboratory methods of studying the mechanical properties of rocks, *Int. Journ. Rock Mech. Min. Sci.*, 6, 43-90.
- Grinat, M., J. Sauer, and W. Sudekum (2004), Self potential measurements during hydraulic fracturing of Bunter sandstones, *Proc. Near Surface, EAGE*, Utrecht, The Netherlands.
- Jouniaux, L., and J-P. Pozzi (1995), Streaming potential and permeability of saturated sandstones under triaxial stress: consequences for electrotelluric anomalies prior to earthquakes, *J. Geophys. Res.*, 100(B6), 10,197-10,209.
- Kawakami, N., and S. Takasugi (1994), SP Monitoring during hydraulic fracturing using the TG-2 well, *European Assoc. of Exploration Geophysicists; 56th meeting and tech. exhibition, Vienna, Austria*.
- Lorne, B., F. Perrier, and J-P. Avouac (1999), Streaming potential measurements 2. Relationship between electrical and hydraulic flow patterns from rock samples during deformation, *J. Geophys. Res.*, 104(B8), 17,879-17,896.
- Marquis, G., M. Darnet, P. Sailhac, and A. K. Singh (2002), Surface electric variations induced by deep hydraulic stimulation: An example from the Soultz HDR site, *Geophys. Res. Lett.*, 29(14).
- Morgan, F. D., E. R. Williams, and T. R. Madden (1989), Streaming potential properties of westerly granite with applications, *J. Geophys. Res.*, 94(B9), 12,449-12,461.
- Middleton, M. F. (1997), Measurements of streaming potential versus applied pressure for porous rocks, *Phys. Chem. Earth*, 22(1-2), 81-86.
- Pritchett, J. W., and T. Ishido (2005), Hydrofracture characterization using downhole electrical monitoring, *Proc. World Geothermal Congress*, Anatolia, Turkey.
- Reppert, P.M., and F.D. Morgan (2003), Temperature-dependent streaming potentials: 2. Laboratory, *J. Geophys. Res.*, 108(B11), 2547.
- von Smoluchowski, M. (1903) Contribution à la théorie de l'endosmose électrique et de quelques phénomènes corrélatifs, *Bulletin International de l'Academie des Sciences de Cracovie*, 8, 182-200.
- Tosha, T., N. Matsushima, and T. Ishido (2003), Zeta potential measured for an intact granite sample at temperatures to 200C, *Geophys. Res. Lett.*, 30(6).
- Wurmstich, B. (1995), 3D self-consistent modeling of streaming potential responses; theory and feasibility of applications in earth sciences, Doctoral Thesis, Texas A&M University, USA.